

# Lattice and phenomenology of the Quark Gluon Plasma

---

**Claudia Ratti**<sup>a,\*</sup>

<sup>a</sup>*Physics Department, University of Houston,  
Houston, TX 77204, USA*

*E-mail:* [cratti@uh.edu](mailto:cratti@uh.edu)

I give an overview of recent results for QCD thermodynamics, based on lattice simulations and other approaches.

*The XVIth Quark Confinement and the Hadron Spectrum Conference (QCHSC24)  
19-24 August, 2024  
Cairns Convention Centre, Cairns, Queensland, Australia*

---

\*Speaker

## 1. Introduction

We live in a unique era to map out the phase diagram of strongly interacting matter and its equation of state. Figure 1 shows that, between the present and future terrestrial and cosmic observatories, we are able to cover the whole phase diagram with experimental observations that, when supported by accurate theoretical predictions, will allow us to answer the following fundamental questions. Do we have a critical point on the phase diagram of strongly interacting matter? What are the degrees of freedom in the vicinity of the phase transition? Where is the transition line at high density? What are the phases of QCD at high density? What is the nature of matter in the core of neutron stars? From collider experiments, data are becoming available from the second Beam Energy Scan at RHIC, which covers collision energies down to 3 GeV and will allow us to reach value of chemical potential up to  $\mu_B \sim 750$  MeV. To explore the low-temperature/high-density phases of matter, terrestrial collider experiments are limited and we need to complement their results with gravitational wave observatories.

Explorations of the phase diagram of QCD have been carried out extensively by both theory and experiment in the past decades. It is known that a low-temperature/low-density hadron gas phase is separated from a high-temperature quark gluon plasma (QGP) phase. At exactly zero density, the transition was shown to be an analytic crossover [1] at around  $T \simeq 155 - 160$  MeV [2–7].

The equation of state of QCD is known with good precision at vanishing density from lattice QCD [8, 9]. Lattice simulations are the main first principles method to investigate the thermodynamics of the theory. Many of the established features of the phase diagram have been determined via lattice simulations, such as the crossover nature of the transition, and its pseudo-critical temperature. Because of the fermion sign problem, direct lattice simulations at non-zero density are extremely costly, and are currently limited to small volumes. Most results on finite-density thermodynamics rely on extrapolations, mainly Taylor expansion or analytic continuation from imaginary chemical potentials. Both currently allow for an exploration of the thermodynamics to small/intermediate densities.

One of the most challenging questions in the field of quantum chromodynamics (QCD) concerns the existence of a first-order phase transition at finite baryon chemical potential  $\mu_B$  and high temperature  $T$ , separating the hadronic and quark-gluon plasma phases. From state of the art lattice QCD calculations, we know that the transition from hadronic matter to deconfined quark gluon plasma at  $\mu_B = 0$  is an analytic, smooth crossover [2], taking place at a pseudocritical temperature of 155 – 158 MeV [7, 10]. Because direct lattice QCD simulations are not feasible at finite density due to the fermion sign problem, whether a first-order phase transition occurs at large chemical potential remains an open question. Extrapolations of lattice results to small baryon densities indicate that the analytic crossover persists at least up to  $\mu_B/T \lesssim 3$  [7, 11, 12], although a hint of a narrowing of the crossover towards large  $\mu_B$  was observed for the first time in [13]. Several effective QCD theories predict a first-order phase transition at large  $\mu_B$ , originating from a critical point (CP) where the transition is of second order (for recent reviews, see [14, 15]). While in the past the theoretical predictions for the location of the QCD critical point were scattered all over the QCD phase diagram, more recent ones seem to concentrate around a considerably narrower region, with chemical potentials in the range  $400 \leq \mu_B \leq 650$  MeV [16–21].

The universal features and peculiar behavior expected near the QCD critical point make a

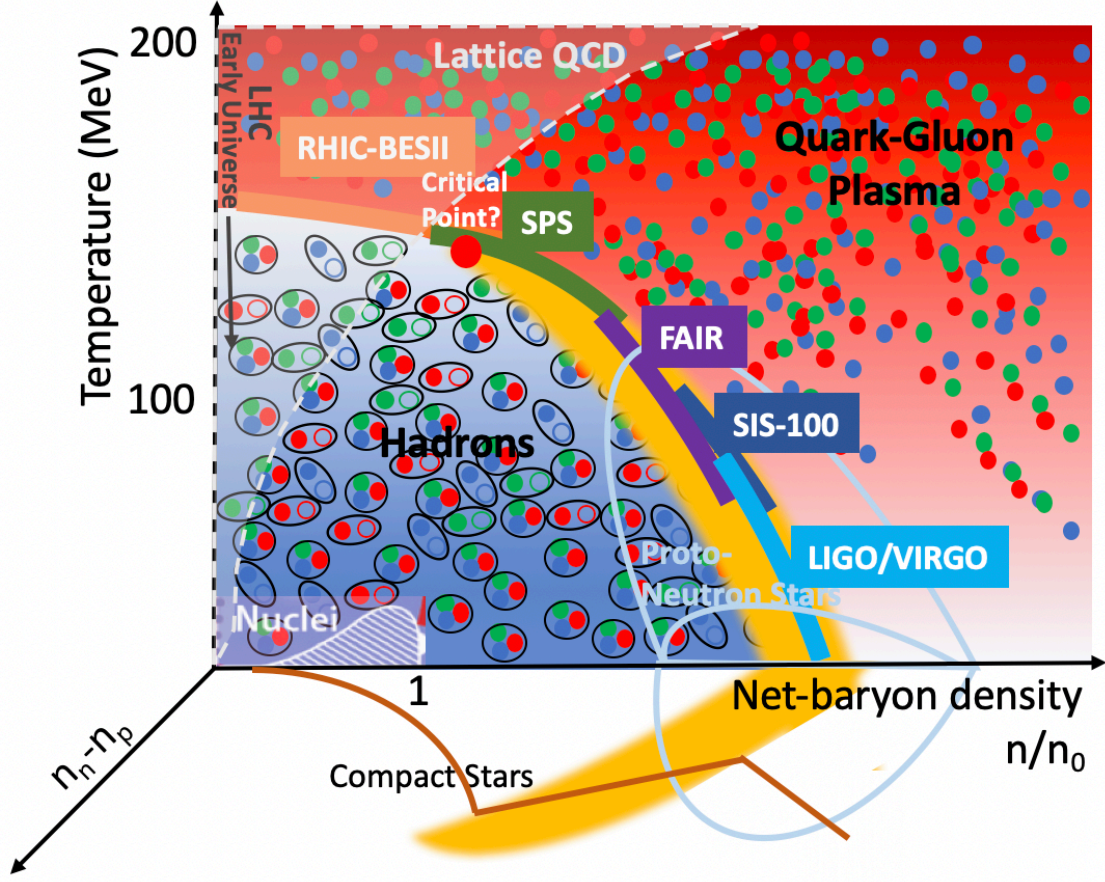


**Figure 1:** Cartoon of the QCD phase diagram in the Temperature  $T$ , scaled net-baryon density  $n/n_0$  and net-isospin density  $n_n - n_p$  phase space.

compelling case for its experimental search in heavy-ion collisions, in particular utilizing event-by-event fluctuations in multiplicities of produced particles [22–24]. The experimental search for the QCD critical point is one of the primary goals of the Beam Energy Scan program at RHIC, which finished its runs in 2021 [14, 25]. Proton cumulants are expected to show characteristic signatures of critical behavior, although interpreting experimental results in this context is challenging. The data from the STAR Collaboration [26, 27], including the new preliminary data from BESII on proton number factorial cumulants [28], hint at an interesting behavior for energies  $\sqrt{s_{NN}} \leq 20$  GeV. These features cannot be explained by non-critical baselines [29, 30], even though no conclusive statement on the critical point existence/location has been made so far either using the proton cumulants, or other considerations such as finite-size scaling [31–33].

## 2. QCD Equation of State at finite density

### 2.1 Results from lattice QCD

For the equation of state, Taylor expansions around  $\mu_B = 0$  up to  $N^4$ LO allow to describe the regime  $\mu_B/T \leq 2.5 - 3$  [34], though at higher densities they typically break down due to the

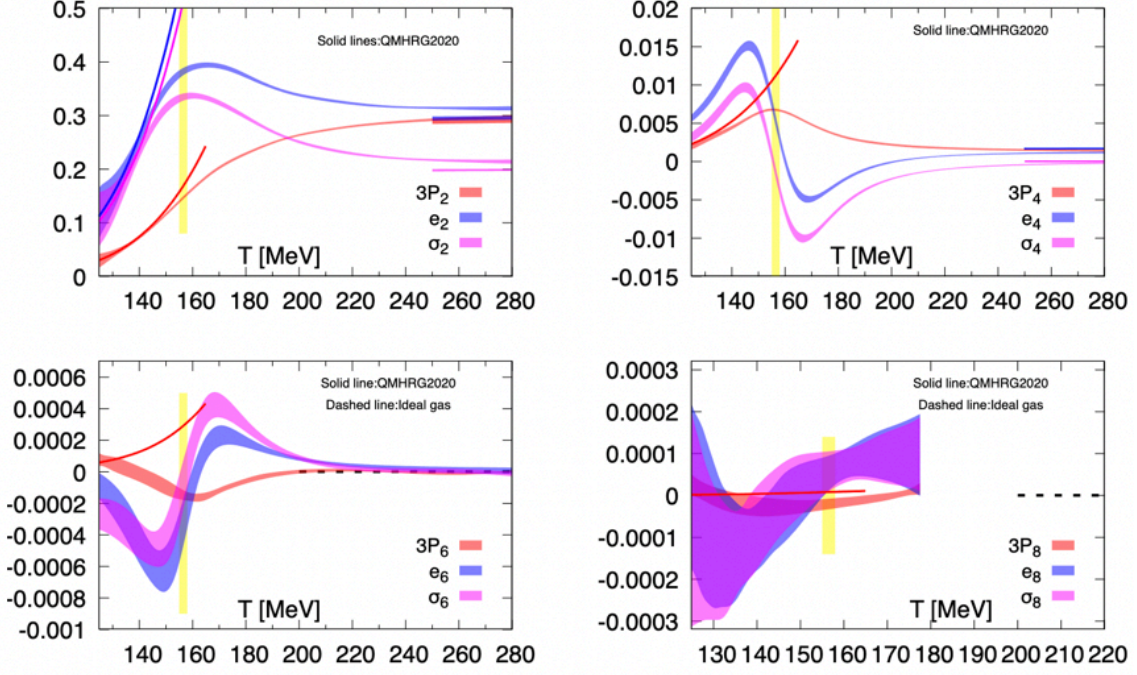


**Figure 2:** From Ref. [34]: Second, fourth, sixth and eighth order Taylor expansion coefficients as functions of the temperature at  $\mu_B = 0$ .

presence of unphysical behavior in some thermodynamic quantities. This is likely due to the fact that the extrapolation is carried out at constant temperature, and is thus forced to cross the transition line at some non-zero  $\mu_B$ . The most recent Taylor expansion coefficients are shown in Fig. 2. They were obtained in Ref. [34]. A more recent analysis, on smaller lattices, was recently performed in Ref. [35].

Recently, an alternative expansion has been developed [36, 37], that instead implements the extrapolation along lines of constant density, thus avoiding crossing the transition. Such alternative scheme allows for extrapolations up to  $\mu_B/T \leq 3.5$ , with small uncertainties and without unphysical behavior. It also shows better convergence properties than Taylor expansions, due to a large separation between the LO and NLO expansion coefficients. Recently, in Ref. [38] the scheme was compared to Taylor expansions in a number of models of QCD matter, showing superior convergence properties around and above the transition temperature, in the  $\mu_B$  direction though not in the hadronic phase. A comparison with direct lattice QCD results at finite chemical potential from reweighting methods was presented in Ref. [39], showing substantial agreement.

Figure 3 shows pressure and entropy density as functions of the temperature, for different values of  $\mu_B/T$ , obtained with the new expansion scheme in Ref. [36].

QCD has three conserved charges: baryon number  $B$ , strangeness  $S$  and electric charge  $Q$ , or isospin  $I$ . For example, in heavy-ion collisions we have zero global strangeness and global electric charge equal to a fraction of the baryon number that reflects the conditions of the colliding nuclei. However, to describe the system created in the collisions, one can use hydrodynamic simulations in which the fluid is split into small cells, and in each one of them  $S$ ,  $Q$  and  $B$  can fluctuate away



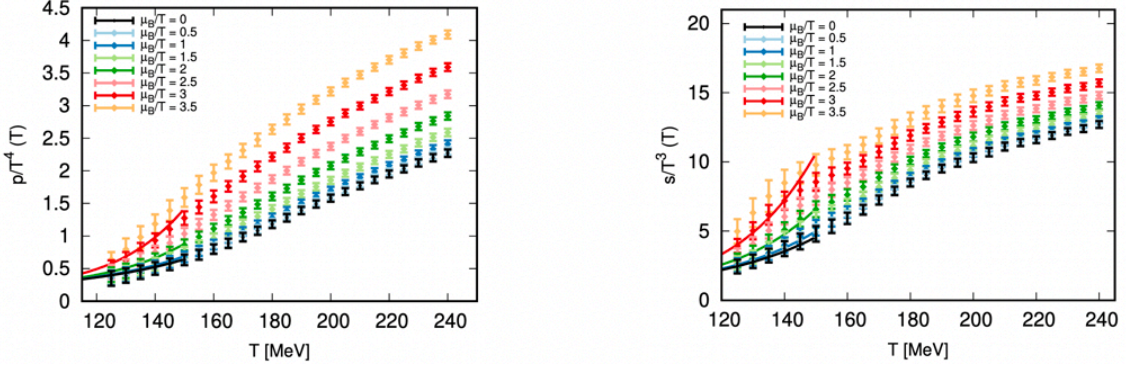


**Figure 3:** From Ref. [36]: Pressure (left) and entropy density (right) as functions of the temperature for different values of  $\mu_B/T$ .

from their global values [40]. At the same time, in neutron stars we have global charge=0 for stability, strangeness is most likely not in equilibrium, and we have an imbalance between protons and neutrons which brings to a finite isospin density. Finally, for the cosmological trajectories, we could have large lepton flavor asymmetries, that would lead to large asymmetries between quark flavors and therefore also to trajectories at finite  $T$ ,  $\mu_B$  and  $\mu_Q$ .

For these reasons, one needs an equation of state as a function of four independent variables:  $T$ ,  $\mu_B$ ,  $\mu_S$ ,  $\mu_Q$ . Two equations of state have been realized, based on a four-dimensional Taylor expansion [41–43] obtained from lattice QCD results from the Wuppertal-Budapest and HotQCD collaborations, respectively. A new version of the 4D equation of state, based on the novel expansion scheme [36], has recently been presented [44].

## 2.2 Towards high densities

QCD cannot be calculated from first principles in the regime relevant for neutron stars and, thus, either effective field theories or microscopic effective models are required to understand dense matter under these conditions. Because of the widely different degrees of freedom and interactions across the different layers of neutron stars, a single, uniform equation of state (EoS) approach does not yet exist [45]. Instead, different regions inside neutron stars (sometimes a single layer or possibly multiple layers) are described with different and separate EoSs, and then matched together where their regimes of validity overlap. In Ref. [46], the MUSES collaboration collected all available constraints, from heavy-ion and astrophysical observation, on the QCD equation of state. An equation of state with a broad density and temperature coverage will have to satisfy several of these constraints in order to be valid.

A major roadblock in understanding the neutron star EoS is that there are many different models, and each one of them has underlying free parameters that can significantly affect their predictions for neutron star properties. A single rendering of an EoS from tuned physical parameters cannot cover the entire allowable phase space for a specific model. Furthermore, many software packages that calculate EoSs are proprietary, such that they are not available to the wider public. Even when they are open source, they may not be user-friendly and/or they may only describe a small region of the star. One approach to begin to tackle these challenges is to store EoS tables in large repositories.

The largest one for astrophysics is called CompOSE [47–50]. CompOSE contains over 300 EoSs that cover different regions of the QCD phase diagram relevant to neutron stars. CompOSE has been very important for pushing forward the dense matter astrophysics field, giving a wider range of physicists across fields access to a broad range of neutron star EoSs using one standardized output [51]. However, because CompOSE is a database and does not include the EoS models themselves, one cannot vary free parameters within EoSs on CompOSE, nor can one edit or modify the EoS models, as new data furthers our knowledge.

The MUSES collaboration was funded with the purpose of providing the community with a software generating several equations of state, covering different regions of the QCD phase diagram, that the users could explore by changing the parameters in a systematic way. In Ref. [52], the MUSES Calculation Engine was introduced, which was built to model the EoS across the QCD phase diagram (including inside neutron stars and during heavy ion collisions) with a variety of relevant models. The EoS modules that currently make up the MUSES CE are the following: Crust Density Functional Theory (Crust-DFT, valid starting at low densities and at neutron star temperatures), Chiral Effective Field Theory ( $\chi$ EFT, valid around saturation density and at zero temperatures in the current version), Chiral Mean Field (CMF, valid beyond saturation density and at zero temperatures in the current version), Lepton (valid at any densities, but zero temperatures in the current version), 4D Taylor-expanded Lattice (BQS, valid at low densities and high temperatures), Ising 2D  $T'$ -Expansion Scheme (TExS, valid at low densities and high temperatures) [53], and Holographic (NumRelHolo, valid across a wide range of densities, but high temperatures). Other modules will become available in the near future.

### 3. QCD Transition line

In a crossover, there is no sudden jump in the first derivatives of the pressure. Nevertheless, a chiral pseudo-phase transition line can be calculated based on where the order parameters change more rapidly. The exact location of the QCD transition line is a hot topic of research in the field of strong interactions. The most recent results are contained in Ref. [7]. The transition temperature, obtained from the chiral condensate and its susceptibility, as a function of the chemical potential can be parametrized as

$$\frac{T_c(\mu_B)}{T_c(\mu_B=0)} = 1 - \kappa_2 \left( \frac{\mu_B}{T_c(\mu_B)} \right)^2 - \kappa_4 \left( \frac{\mu_B}{T_c(\mu_B)} \right)^4 + \dots \quad (1)$$

The crossover or pseudo-critical temperature  $T_c$  has been determined with extreme accuracy and extrapolated from imaginary up to real  $\mu_B \approx 300$  MeV. Additionally, the width of the chiral transition and the peak value of the chiral susceptibility were calculated along the crossover line. Both of them are constant functions of  $\mu_B$ . This means that, up to  $\mu_B = 300$  MeV, no sign of criticality has been observed in lattice results. In fact, at the critical point the height of the peak of the chiral susceptibility would diverge and its width would shrink. The small error reflects the most precise determination of the  $T - \mu_B$  phase transition line using lattice techniques. Besides  $T_c = 158 \pm 0.6$  MeV, the study provides updated results for the coefficients  $\kappa_2 = 0.0153 \pm 0.0018$  and  $\kappa_4 = 0.00032 \pm 0.00067$  [7]. Similar coefficients for the extrapolation of the transition temperature to finite strangeness, electric charge, and isospin chemical potentials were obtained in Ref. [10], and are displayed in Table 1.

| $\kappa_2^B$ | $\kappa_4^B$ | $\kappa_2^S$ | $\kappa_4^S$ | $\kappa_2^Q$ | $\kappa_4^Q$ | $\kappa_2^I$ | $\kappa_4^I$ |
|--------------|--------------|--------------|--------------|--------------|--------------|--------------|--------------|
| 0.016(6)     | 0.001(7)     | 0.017(5)     | 0.004(6)     | 0.029(6)     | 0.008(1)     | 0.026(4)     | 0.005(7)     |

**Table 1:** Continuum-extrapolated values of  $\kappa_2^X$  and  $\kappa_4^X$  (with  $\mu_Q = \mu_S = 0$  for  $X = B$ ,  $\mu_B = \mu_Q = 0$  for  $X = S$  and  $\mu_B = \mu_S = 0$  for  $X = Q, I$ ) from [10].

#### 4. Critical point estimates from lattice QCD and other approaches

As mentioned in the previous section, in Ref. [7], by extrapolating the proxy for the transition width as well as the height of the chiral susceptibility peak from imaginary to real  $\mu_B$ , the strength of the phase transition was evaluated and no indication of criticality was found up to  $\mu_B \approx 300$  MeV. On the other hand, a phase transition temperature at  $\mu_B = 0$  of  $T_c = 132_{-6}^{+3}$  MeV was found in the chiral limit by the HotQCD collaboration using lattice QCD calculations with “rooted” staggered fermions [54]. This transition temperature is computed with two massless light quarks and a physical strange quark based on two unique estimators. Since the curvature of the phase diagram is negative, a critical point in the chiral limit would sit at a temperature smaller than this one. The expectation is that the temperature of the critical point at physical quark masses has to be smaller than the one of the critical point in the chiral limit, and therefore definitely smaller than  $T_c = 132_{-6}^{+3}$  MeV.

Several recent predictions for the location of the critical point have been obtained via functional methods [16–18, 55–57], holography [19, 58, 59] and the analysis of experimental data [31, 33, 60, 61]. Many (but not all) of these predictions based on different approaches cluster in a rather small region on the QCD phase diagram. Figure 4 shows a collection of these critical points on the QCD phase diagram. Out of these approaches, I will focus here on a few that I was directly involved with.

In the first project, we use a holographic approach [63] to extrapolate lattice QCD information from zero to large baryon chemical potential  $\mu_B$ . This model is a natural good candidate, since it can reproduce lattice QCD results at low densities, where they are available [58, 64], and naturally leads to the almost ideal-fluid behavior of the Quark-Gluon Plasma [65], as observed in experiments. We use a Bayesian analysis, and two functional forms for the potential and coupling functions that are the main unknown in our model, to perform a systematic scan of the parameters, constrained by lattice QCD results at zero density [66, 67], with a probability given by the respective error bars. Our predictions for the QCD critical point, based on the posterior parameter distributions, agree within one sigma for the two model realizations, and collapse to a very small region of the phase diagram, which is within the phase transition band from lattice QCD simulations [19].

In Ref. [68] a novel method, based solely on lattice results, was proposed to estimate the location of the critical point by studying contours of constant entropy density on the QCD phase diagram. The idea is to employ the entropy contours to search for the onset of a first order regime: if different contours meet somewhere in the phase diagram, it means that the entropy has become multi-valued, hence the transition has turned first order. By determining where the first order regime is reached, the location of the critical point can be estimated. In Ref. [68], the entropy contours were constructed based on existing lattice results at vanishing chemical potential for the entropy density [66] and second order baryon susceptibility [36]. The prediction for the location of the critical point from this analysis is indicated by the two ellipses in Fig. 4, the red one corresponding

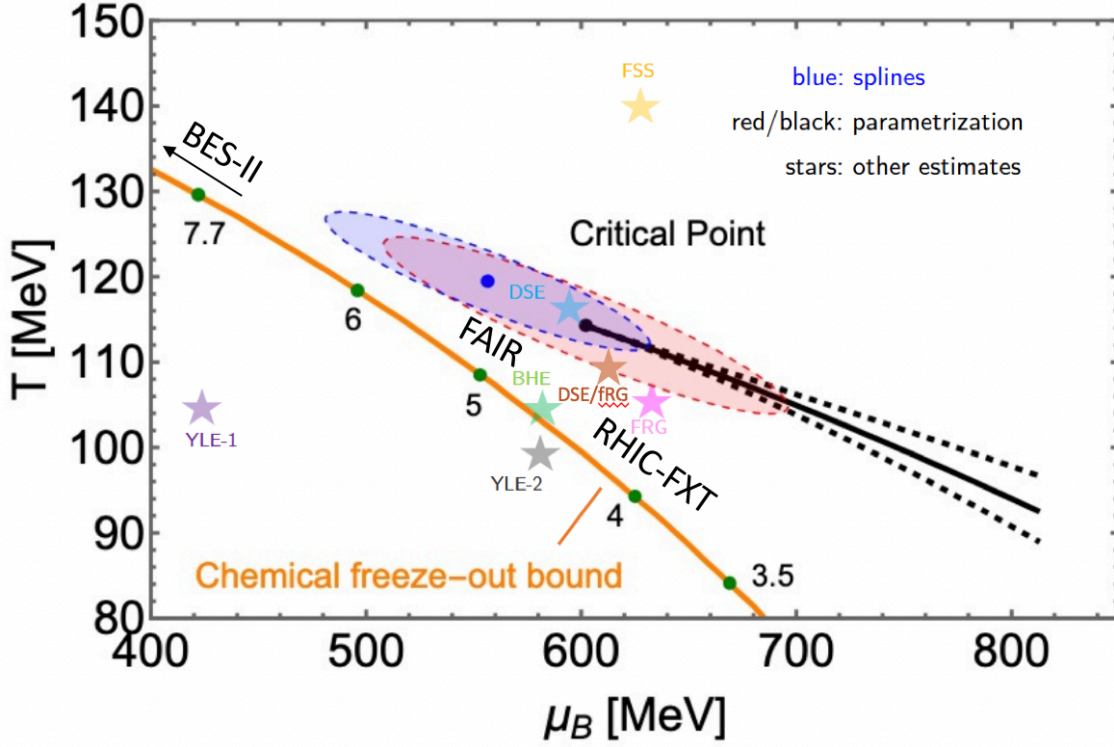


**Figure 4:** Compilation of critical points from the literature from Refs. [16–19, 33, 55–57]. Also shows is the chemical freeze-out line from Ref. [62], to be considered a lower bound for the critical point location.

to a parameterization and the blue one to a spline fit of the lattice QCD results.

In Ref. [69], we generalized the method described above in more than one way. To reach the necessary precision to bear predictive power, we performed a new computation of the equation of state of QCD at zero density, with significantly reduced uncertainties compared to existing results. Instead of extracting the constant entropy contours from  $\mu_B = 0$  data, we extrapolated them from imaginary  $\mu_B$ . In addition, we increased the statistics of data sets at the three highest imaginary chemical potentials on the finest lattice in comparison to our earlier work [37]. While the extrapolation in Ref. [68] was done at order  $\mathcal{O}(\mu_B^2)$ , we allowed for leading corrections to the linear  $\mu_B^2$  dependence. We used the actual statistical correlations between variables and also considered additional sources of systematic errors in the analysis. Besides, the results presented in Ref. [68] were obtained for zero strangeness chemical potential, while in Ref. [69] we enforce strangeness neutrality. We were thus able to determine an exclusion probability for the existence of a critical point as a function of the chemical potential. We found that, at the  $2\sigma$  level, we can exclude the existence of a critical point below  $\mu_B^{2\sigma} = 450$  MeV.

## 5. Conclusions

In this contribution, I discussed the current state of the art of lattice QCD results on the equation of state and phase diagram, where there is a continued effort to extend the coverage in



density. New equations of state are becoming available, with extended coverage in density and additional dependence on strangeness and electric charge chemical potentials.

To reach the densities needed to describe the lowest collision energies in colliders, or even more neutron star mergers, we need to complement first principle results with more phenomenological approaches. We need to constrain the parameters of these approaches through systematic analyses of experimental data, combine with astrophysical observations. With new data from accelerator facilities and future gravitational wave observatories, this will hopefully become possible in the near future.

## References

- [1] Y. Aoki, G. Endrodi, Z. Fodor, S.D. Katz and K.K. Szabo, *The Order of the quantum chromodynamics transition predicted by the standard model of particle physics*, *Nature* **443** (2006) 675 [[hep-lat/0611014](#)].
- [2] Y. Aoki, Z. Fodor, S.D. Katz and K.K. Szabo, *The QCD transition temperature: Results with physical masses in the continuum limit*, *Phys. Lett. B* **643** (2006) 46 [[hep-lat/0609068](#)].
- [3] Y. Aoki, S. Borsanyi, S. Durr, Z. Fodor, S.D. Katz, S. Krieg et al., *The QCD transition temperature: results with physical masses in the continuum limit II.*, *JHEP* **06** (2009) 088 [[0903.4155](#)].
- [4] WUPPERTAL-BUDAPEST collaboration, *Is there still any  $T_c$  mystery in lattice QCD? Results with physical masses in the continuum limit III*, *JHEP* **09** (2010) 073 [[1005.3508](#)].
- [5] A. Bazavov et al., *The chiral and deconfinement aspects of the QCD transition*, *Phys. Rev. D* **85** (2012) 054503 [[1111.1710](#)].
- [6] HotQCD collaboration, *Chiral crossover in QCD at zero and non-zero chemical potentials*, *Phys. Lett. B* **795** (2019) 15 [[1812.08235](#)].
- [7] S. Borsanyi, Z. Fodor, J.N. Guenther, R. Kara, S.D. Katz, P. Parotto et al., *QCD Crossover at Finite Chemical Potential from Lattice Simulations*, *Phys. Rev. Lett.* **125** (2020) 052001 [[2002.02821](#)].
- [8] S. Borsanyi, Z. Fodor, S. Katz, S. Krieg, C. Ratti and K. Szabo, *Freeze-out parameters: lattice meets experiment*, *Phys. Rev. Lett.* **111** (2013) 062005 [[1305.5161](#)].
- [9] HotQCD collaboration, *Equation of state in (2+1)-flavor QCD*, *Phys. Rev. D* **90** (2014) 094503 [[1407.6387](#)].
- [10] HotQCD collaboration, *Chiral crossover in QCD at zero and non-zero chemical potentials*, *Phys. Lett. B* **795** (2019) 15 [[1812.08235](#)].
- [11] V. Vovchenko, J. Steinheimer, O. Philipsen and H. Stoecker, *Cluster Expansion Model for QCD Baryon Number Fluctuations: No Phase Transition at  $\mu_B/T < \pi$* , *Phys. Rev. D* **97** (2018) 114030 [[1711.01261](#)].

- [12] HotQCD collaboration, *Taylor expansions and Padé approximants for cumulants of conserved charge fluctuations at nonvanishing chemical potentials*, *Phys. Rev. D* **105** (2022) 074511 [2202.09184].
- [13] S. Borsanyi, Z. Fodor, J.N. Guenther, P. Parotto, A. Pasztor, L. Pirelli et al., *QCD deconfinement transition line up to  $\mu_B = 400$  MeV from finite volume lattice simulations*, 2410.06216.
- [14] A. Bzdak, S. Esumi, V. Koch, J. Liao, M. Stephanov and N. Xu, *Mapping the Phases of Quantum Chromodynamics with Beam Energy Scan*, *Phys. Rept.* **853** (2020) 1 [1906.00936].
- [15] L. Du, A. Sorensen and M. Stephanov, *The QCD phase diagram and Beam Energy Scan physics: a theory overview*, 2, 2024, DOI [2402.10183].
- [16] W.-j. Fu, J.M. Pawłowski and F. Rennecke, *QCD phase structure at finite temperature and density*, *Phys. Rev. D* **101** (2020) 054032 [1909.02991].
- [17] P.J. Gunkel and C.S. Fischer, *Locating the critical endpoint of QCD: Mesonic backcoupling effects*, *Phys. Rev. D* **104** (2021) 054022 [2106.08356].
- [18] F. Gao and J.M. Pawłowski, *Chiral phase structure and critical end point in QCD*, *Phys. Lett. B* **820** (2021) 136584 [2010.13705].
- [19] M. Hippert, J. Grefa, T.A. Manning, J. Noronha, J. Noronha-Hostler, I. Portillo Vazquez et al., *Bayesian location of the QCD critical point from a holographic perspective*, 2309.00579.
- [20] G. Basar, *QCD critical point, Lee-Yang edge singularities, and Padé resummations*, *Phys. Rev. C* **110** (2024) 015203 [2312.06952].
- [21] D.A. Clarke, P. Dimopoulos, F. Di Renzo, J. Goswami, C. Schmidt, S. Singh et al., *Searching for the QCD critical endpoint using multi-point Padé approximations*, 2405.10196.
- [22] M.A. Stephanov, K. Rajagopal and E.V. Shuryak, *Event-by-event fluctuations in heavy ion collisions and the QCD critical point*, *Phys. Rev. D* **60** (1999) 114028 [hep-ph/9903292].
- [23] Y. Hatta and M.A. Stephanov, *Proton number fluctuation as a signal of the QCD critical endpoint*, *Phys. Rev. Lett.* **91** (2003) 102003 [hep-ph/0302002].
- [24] M.A. Stephanov, *Non-Gaussian fluctuations near the QCD critical point*, *Phys. Rev. Lett.* **102** (2009) 032301 [0809.3450].
- [25] X. Luo and N. Xu, *Search for the QCD Critical Point with Fluctuations of Conserved Quantities in Relativistic Heavy-Ion Collisions at RHIC : An Overview*, *Nucl. Sci. Tech.* **28** (2017) 112 [1701.02105].
- [26] STAR collaboration, *Nonmonotonic Energy Dependence of Net-Proton Number Fluctuations*, *Phys. Rev. Lett.* **126** (2021) 092301 [2001.02852].

- [27] STAR collaboration, *Cumulants and correlation functions of net-proton, proton, and antiproton multiplicity distributions in Au+Au collisions at energies available at the BNL Relativistic Heavy Ion Collider*, *Phys. Rev. C* **104** (2021) 024902 [2101.12413].
- [28] A. Pandav [for STAR collaboration], 2024.
- [29] P. Braun-Munzinger, B. Friman, K. Redlich, A. Rustamov and J. Stachel, *Relativistic nuclear collisions: Establishing a non-critical baseline for fluctuation measurements*, *Nucl. Phys. A* **1008** (2021) 122141 [2007.02463].
- [30] V. Vovchenko, V. Koch and C. Shen, *Proton number cumulants and correlation functions in Au-Au collisions at  $\sqrt{s_{NN}}=7.7\text{--}200$  GeV from hydrodynamics*, *Phys. Rev. C* **105** (2022) 014904 [2107.00163].
- [31] E.S. Fraga, L.F. Palhares and P. Sorensen, *Finite-size scaling as a tool in the search for the QCD critical point in heavy ion data*, *Phys. Rev. C* **84** (2011) 011903 [1104.3755].
- [32] R.A. Lacey, *Indications for a Critical End Point in the Phase Diagram for Hot and Dense Nuclear Matter*, *Phys. Rev. Lett.* **114** (2015) 142301 [1411.7931].
- [33] A. Sorensen and P. Sorensen, *Locating the critical point for the hadron to quark-gluon plasma phase transition from finite-size scaling of proton cumulants in heavy-ion collisions*, 2405.10278.
- [34] HotQCD collaboration, *Equation of state and speed of sound of (2+1)-flavor QCD in strangeness-neutral matter at nonvanishing net baryon-number density*, *Phys. Rev. D* **108** (2023) 014510 [2212.09043].
- [35] S. Borsanyi, Z. Fodor, J.N. Guenther, S.D. Katz, P. Parotto, A. Pasztor et al., *Continuum-extrapolated high-order baryon fluctuations*, *Phys. Rev. D* **110** (2024) L011501 [2312.07528].
- [36] S. Borsányi, Z. Fodor, J.N. Guenther, R. Kara, S.D. Katz, P. Parotto et al., *Lattice QCD equation of state at finite chemical potential from an alternative expansion scheme*, *Phys. Rev. Lett.* **126** (2021) 232001 [2102.06660].
- [37] S. Borsanyi, J.N. Guenther, R. Kara, Z. Fodor, P. Parotto, A. Pasztor et al., *Resummed lattice QCD equation of state at finite baryon density: Strangeness neutrality and beyond*, *Phys. Rev. D* **105** (2022) 114504 [2202.05574].
- [38] M. Kahangirwe, I. Gonzalez, J.A. Muñoz, C. Ratti and V. Vovchenko, *Convergence properties of  $T'$ -Expansion Scheme: Hadron Resonance Gas and Cluster Expansion Model*, 2408.04588.
- [39] S. Borsanyi, Z. Fodor, M. Giordano, J.N. Guenther, S.D. Katz, A. Pasztor et al., *Equation of state of a hot-and-dense quark gluon plasma: Lattice simulations at real  $\mu_B$  vs extrapolations*, *Phys. Rev. D* **107** (2023) L091503 [2208.05398].

- [40] C. Plumberg et al., *BSQ Conserved Charges in Relativistic Viscous Hydrodynamics solved with Smoothed Particle Hydrodynamics*, [2405.09648](#).
- [41] J. Noronha-Hostler, P. Parotto, C. Ratti and J.M. Stafford, *Lattice-based equation of state at finite baryon number, electric charge and strangeness chemical potentials*, *Phys. Rev. C* **100** (2019) 064910 [[1902.06723](#)].
- [42] A. Monnai, B. Schenke and C. Shen, *Equation of state at finite densities for QCD matter in nuclear collisions*, *Phys. Rev. C* **100** (2019) 024907 [[1902.05095](#)].
- [43] A. Monnai, G. Pihan, B. Schenke and C. Shen, *Four-dimensional QCD equation of state with multiple chemical potentials*, *Phys. Rev. C* **110** (2024) 044905 [[2406.11610](#)].
- [44] A. Abuali, S. Borsányi, Z. Fodor, J. Jahan, M. Kahangirwe, P. Parotto et al., *A new 4D lattice QCD equation of state: extended density coverage from a generalized  $T'$ -expansion*, [2504.01881](#).
- [45] V. Dexheimer, J. Noronha, J. Noronha-Hostler, C. Ratti and N. Yunes, *Future physics perspectives on the equation of state from heavy ion collisions to neutron stars*, *J. Phys. G* **48** (2021) 073001 [[2010.08834](#)].
- [46] MUSES collaboration, *Theoretical and experimental constraints for the equation of state of dense and hot matter*, *Living Rev. Rel.* **27** (2024) 3 [[2303.17021](#)].
- [47] M. Oertel, M. Hempel, T. Klähn and S. Typel, *Equations of state for supernovae and compact stars*, *Rev. Mod. Phys.* **89** (2017) 015007 [[1610.03361](#)].
- [48] S. Typel, M. Oertel and T. Klähn, *CompOSE CompStar online supernova equations of state harmonising the concert of nuclear physics and astrophysics compose.obspm.fr*, *Phys. Part. Nucl.* **46** (2015) 633 [[1307.5715](#)].
- [49] COMPOSE CORE TEAM collaboration, *CompOSE Reference Manual*, *Eur. Phys. J. A* **58** (2022) 221 [[2203.03209](#)].
- [50] “CompOSE: CompStar Online Supernova Equations of state website.”
- [51] V. Dexheimer, M. Mancini, M. Oertel, C. Providência, L. Tolos and S. Typel, *Quick Guides for Use of the CompOSE Data Base*, *Particles* **5** (2022) 346 [[2311.04715](#)].
- [52] M. Reinke Pelicer et al., *Building Neutron Stars with the MUSES Calculation Engine*, [2502.07902](#).
- [53] M. Kahangirwe, S.A. Bass, J. Jahan, P. Moreau, P. Parotto, C. Ratti et al., *Lattice-based equation of state with 3D Ising critical point*, *12*, 2023 [[2312.11265](#)].
- [54] HOTQCD collaboration, *Chiral Phase Transition Temperature in (2+1)-Flavor QCD*, *Phys. Rev. Lett.* **123** (2019) 062002 [[1903.04801](#)].



- [55] P. Isserstedt, M. Buballa, C.S. Fischer and P.J. Gunkel, *Baryon number fluctuations in the QCD phase diagram from Dyson-Schwinger equations*, *Phys. Rev. D* **100** (2019) 074011 [[1906.11644](#)].
- [56] F. Gao and J.M. Pawłowski, *QCD phase structure from functional methods*, *Phys. Rev. D* **102** (2020) 034027 [[2002.07500](#)].
- [57] W.-j. Fu, X. Luo, J.M. Pawłowski, F. Rennecke, R. Wen and S. Yin, *Hyper-order baryon number fluctuations at finite temperature and density*, *Phys. Rev. D* **104** (2021) 094047 [[2101.06035](#)].
- [58] R. Critelli, J. Noronha, J. Noronha-Hostler, I. Portillo, C. Ratti and R. Rougemont, *Critical point in the phase diagram of primordial quark-gluon matter from black hole physics*, *Phys. Rev. D* **96** (2017) 096026 [[1706.00455](#)].
- [59] L. Zhu, X. Chen, K. Zhou, H. Zhang and M. Huang, *Bayesian Inference of the Critical Endpoint in 2+1-Flavor System from Holographic QCD*, [2501.17763](#).
- [60] R.A. Lacey, *Indications for a critical point in the phase diagram for hot and dense nuclear matter*, *Nucl. Phys. A* **956** (2016) 348 [[1512.09152](#)].
- [61] J. Steinheimer, M. Omana Kuttan, T. Reichert, Y. Nara and M. Bleicher, *Predicting the QCD critical point and EoS from combining HIC and neutron star observations*, [2501.12849](#).
- [62] A. Lysenko, M.I. Gorenstein, R. Poberezhniuk and V. Vovchenko, *Chemical freeze-out curve in heavy-ion collisions and the QCD critical point*, [2408.06473](#).
- [63] R. Rougemont, J. Grefa, M. Hippert, J. Noronha, J. Noronha-Hostler, I. Portillo et al., *Hot QCD phase diagram from holographic Einstein–Maxwell–Dilaton models*, *Prog. Part. Nucl. Phys.* **135** (2024) 104093 [[2307.03885](#)].
- [64] J. Grefa, J. Noronha, J. Noronha-Hostler, I. Portillo, C. Ratti and R. Rougemont, *Hot and dense quark-gluon plasma thermodynamics from holographic black holes*, *Phys. Rev. D* **104** (2021) 034002 [[2102.12042](#)].
- [65] J. Grefa, M. Hippert, J. Noronha, J. Noronha-Hostler, I. Portillo, C. Ratti et al., *Transport coefficients of the quark-gluon plasma at the critical point and across the first-order line*, *Phys. Rev. D* **106** (2022) 034024 [[2203.00139](#)].
- [66] S. Borsanyi, Z. Fodor, C. Hoelbling, S.D. Katz, S. Krieg and K.K. Szabo, *Full result for the QCD equation of state with 2+1 flavors*, *Phys. Lett. B* **730** (2014) 99 [[1309.5258](#)].
- [67] R. Bellwied, S. Borsanyi, Z. Fodor, S.D. Katz, A. Pasztor, C. Ratti et al., *Fluctuations and correlations in high temperature QCD*, *Phys. Rev. D* **92** (2015) 114505 [[1507.04627](#)].
- [68] H. Shah, M. Hippert, J. Noronha, C. Ratti and V. Vovchenko, *Locating the QCD critical point from first principles through contours of constant entropy density*, [2410.16206](#).
- [69] S. Borsanyi, Z. Fodor, J.N. Guenther, P. Parotto, A. Pasztor, C. Ratti et al., *Lattice QCD constraints on the critical point from an improved precision equation of state*, [2502.10267](#).